

Grid Integration of a Renewable Energy System: Modeling and Analysis

Shaimaa Omran *‡, Robert Broadwater **

* Engineering Research Division, National Research Centre, El Buhouth st., Dokki, Cairo,12622, Egypt

**Electrical and Computer Engineering Department, Virginia Tech, Blacksburg, VA 24061, USA

**Electrical Distribution Design (EDD), Blacksburg, VA 24061 USA

(shmomran@vt.edu, dew@vt.edu)

‡Corresponding Author; Shaimaa Omran, Engineering Research Division, National Research Centre, El Buhouth st., Dokki, Cairo,12622, Egypt, Tel: +201067813566, shmomran@vt.edu

Received: 09.07.2020 Accepted:07.08.2020

Abstract- This paper presents a study of a steady-state stability analysis with integrating a wind turbine to a standard power network, where an open-source software is used to model the system. The IEEE 9 bus system is simulated using the OpenModelica software. The steady-state stability analysis study of the system is performed with and without using an Automatic Voltage Regulator (AVR) and Speed Governor (GOV) controllers. The steady-state impact of integrating a wind turbine is investigated. Moreover, the voltage dependency of the wind turbine power is examined. The significance of the analysis results provided by the OpenModelica software is discussed. The open-source software OpenModelica application in this study proved to be a user friendly software that is capable of modelling and analyzing a power system network in a timely manner.

Keywords Wind energy; Power system stability; Renewable integration; Automatic voltage regulator; Speed governor controller.

1. Introduction

The wind energy industry has expanded widely over the last 20 years. It initially started growing in Europe and the USA. The growth continued, and recently Asia and the USA are experiencing the most rapid and wide expansion. According to the Global Wind Energy Council (GWEC) 2019 annual report [1], wind installation boomed in 2018, reaching total new installations of 60.4 GW. This implies that the year 2019 is the largest second year in history, after 2015, for new wind installations [1, 2]. Moreover, it is expected that the industry will witness a robust continued growth. This is depicted in Fig.1, showing an expected average of 4% Compound Annual Growth Rate (CAGR) of onshore and offshore new wind installation capacity for the coming 5 years. It is worth noting that this is a pre-COVID outlook of the market; thus, the COVID impacts on the market are still to be assessed. Wind power is and will continue to play, a major role in fulfilling a low carbon energy market and reducing emissions worldwide.

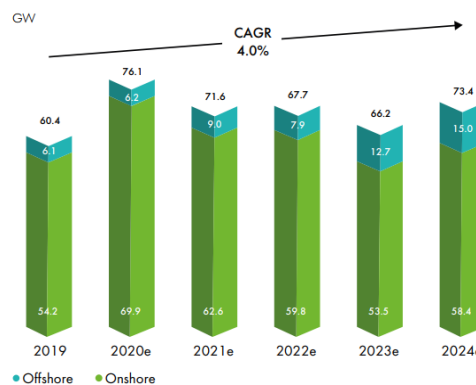


Fig. 1. GWEC new installations expectations for the wind market for the following 5 years [1]

In addition, the wind industry is continuously progressing so as to reduce the levelized cost of electricity, which is considered an accomplishment that strengthens the role of the wind industry [1]. This vital role and increased growth of wind energy introduce challenges to its integration in the power system.

The main contribution of this paper is to elucidate how to use an open-source software to model the studied network with its various components, including controllers, and a renewable energy resource, which is the wind turbine. The steady-state impact of integrating a wind turbine is investigated. Moreover, the voltage dependency of the wind turbine power is examined. The computation time for the voltage dependency study is recorded to investigate the impact of the increase in complexity of the formulas governing the wind turbine power voltage dependencies on the computation time. The rest of the paper is organized as follows. Section 2 presents a literature review of the recent relevant research work. Section 3 provides the methodology used, a description of the proposed system and its model, and an analysis with and without controllers using the OpenModelica software. Section 4 presents an analysis of the model with wind turbine integration. The wind turbine power voltage dependency of the system is also investigated. Finally, section 5 concludes the paper.

2. Literature review

Several research works were conducted to address the different wind power generation technical and operational challenges due to the intermittency of the wind energy resource [3-35]. These challenges include sustaining the voltage and frequency of the power system at stable values during intermittent and fluctuating conditions of the wind resource. In [3] a steady-state analysis is presented for a transmission system with integrated renewable energy resources including 4 wind turbines. Also, a fault is introduced in the system to study the dynamic behavior of the network with renewable integration. The PSSE software is used for the simulation. Moreover, [4] proposes innovative technologies and discusses operation techniques for large scale, distributed wind power. Furthermore, [5] describes the technical challenges of the penetration of renewable energies in the distribution network as well as the transmission network. It addresses specifically the challenges associated with wind integration in the transmission network, such as voltage stability, rotor angle stability, frequency stability, and planning of ancillary services. In addition, [6] provides a description of wind energy technologies, different types of wind turbines, the power flow model of wind turbines, and the challenges facing implementation and integration of wind energy systems. In [7] a wind farm is simulated and analyzed as an isolated model as well as a grid integrated model using Simulink software. The analysis addressed the wind generator instabilities via symmetrical, asymmetrical, and dynamic voltage tests. In [8] a steady-state stability study of a weak distribution system is performed with and without the integration of a double fed, induction generator, wind farm. Transient stability for faults as 3 phase faults and unexpected load tripping is also performed. The simulation is done using the DigSilent PowerFactory software. Moreover, [9]

investigates how the integration of wind power generator into a 37-bus radial system impacts the operation, with a focus on analyzing the steady-state bus voltages stability. The PSAT-Matlab software is used for simulating the system with and without various levels of wind power penetration. In [10] the impact of grid-connected wind power on the active power, reactive power and power factor of the power system is assessed. The effect of the grid-connected wind power on the system stability is also analyzed. Additionally, [11] studies the effect of wind power uncertainty and fluctuation on the accuracy and stability of the reactive voltage of the grid. The paper proposes a partitioning method of the grid voltage for analyzing the stability of the system. In the present work, a steady-state stability analysis study of the standard IEEE 9 bus network is performed with and without using Automatic Voltage Regulator (AVR) and Speed Governor (GOV) controllers. This analysis considers the stability of the system with and without the integration of a wind turbine. In [19] the authors assess the voltage stability of the power system with increased penetration of renewable wind energy. The voltage stability limit is determined using the active power voltage analysis. The analysis is carried out with increased wind penetration in the grid under normal and contingency operations. The IEEE 14 bus system is simulated using DigSilent PowerFactory software for validation. Also, [20] presents a method to attain the bus voltage stability for power systems with wind power penetration. The paper proposes a line index method to determine the weak buses in the system where voltage drops lead to bus voltage instability, and corrective actions to compensate for serious voltage drops. Validation of the line index method is performed by simulating the IEEE 14 bus system using the PSAT. In [21], the authors investigate the effects and influence of the increase of wind energy penetration on the stability of the power system. The small signal stability of a power system with an integrated wind power plant is evaluated using the eigenvalue analysis. An automatic voltage regulator and a power system stabilizer are added to the system and different combinations of both are used to alleviate the undesirable variations and alterations. Likewise, [22] proposes a key performance indicator as a tool to assess the frequency stability for power systems with a high share of integrated wind power generators. The proposed indicator estimates the frequency performance change, and analyses the effect of fast frequency response by introducing a droop based controller for the wind generators. Besides, [23] proposes a method for a small-signal stability analysis of power systems due to the variability of the output power from the offshore wind power plants. The voltage stability is assessed using an extended Prony analysis, and the frequency stability is assessed using a swing based frequency response metric. Additionally, in [24, 25] the transient stability analysis for a large scale power system with integrated off shore wind farms is addressed. A method is developed to assess the voltage stability, rotor angle stability, and frequency response, taking into consideration the intermittency of the wind power plants and the type of faults experienced in the system. In [24] short term faults are considered in the study; whereas, in [25] the long term faults are discussed. Furthermore, [26] evaluates the unstable behavior of the power system with high integration of wind parks using a voltage stability index. This is an impedance

based stability index that can accurately detect the voltage collapse, specially after a contingency occurs. In addition, [27] proposes a planning model that coordinates the planning problem of wind power plant integration and the transmission network planning problem. The model takes into consideration the static voltage stability as an operational constraint to deal with the voltage issue of large-scale wind farms in the planning stage. Moreover, [28] overviews the probabilistic methods used for studying the small signal stability analysis of the power system integrated with large scale wind power, where the modelling of the dependence and correlation between different wind power sources is considered. Also, [29] proposes a method to overcome the impact of the fluctuations of wind power plant connected to the grid and the imbalance between production and demand; first, by using a micro-grid based wind farm that is connected to the electricity grid. Moreover, a multicellular inverter is deployed rather than the two-level inverter so as to avoid its limitations of introducing voltage output with high ripples.

3. Methodology and analysis

In this section, a brief illustration of power system stability swing equation is introduced. The IEEE 9 bus system is constructed using the OpenModelica open-source software [36]. A steady state stability analysis is then performed. The effect of a step increase in load on the system is analyzed. Afterwards, the impact of using the AVR and GOV controllers is investigated.

3.1. Power System Stability

The operating condition of the power system is considered in steady state when all the measured/calculated quantities that describe the operating condition are considered constant for the analysis. Stability of the system can be categorized to (a) steady-state stability, (b) transient stability, and (c) dynamic stability. Steady-state stability of the power system is the ability of the system to remain in the same steady state operating condition, even after a small disturbance. However, if the system experiences a large disturbance and then returns to a significantly different but acceptable steady state operating condition, then the system is said to be transient stable. Hence, the steady state stability studies investigate the stability of the system under incremental disturbances. The nonlinear equations of the system are approximated and replaced by a set of linear equations that are solved using linear analysis methods to determine the steady state stability of the system. The objective in all stability studies is to examine whether the rotor of the machines return to constant speed after the disturbance [37-39].

The synchronous rotor motion equation is formulated such that the accelerating torque is equal to the moment of inertia of the rotor multiplied by the angular acceleration.

$$J \frac{d^2 \theta_m}{dt^2} = T_a = T_m - T_e \quad \text{N.m.} \quad (1)$$

where

J is the inertia of the rotor in kg.m²

θ_m is the angular displacement of the rotor with respect to a stationary axis in mechanical radians

t is the time in seconds

T_m is the mechanical torque supplied by the prime mover in N.m.

T_e is the electromagnetic torque in N.m.

T_a is the accelerating torque in N.m.

For steady state operation T_m equals T_e and T_a is zero.

$$\theta_m = \omega_{sm} t + \delta_m \quad (2)$$

where ω_{sm} is the synchronous speed of the generator in rad/s and δ_m is the angular displacement of the rotor in mechanical radians.

Derivatives of Eq. (2) are:

$$\frac{d \theta_m}{dt} = \omega_{sm} + \frac{d \delta_m}{dt} \quad (3)$$

$$\frac{d^2 \theta_m}{dt^2} = \omega_{sm} + \frac{d^2 \delta_m}{dt^2} \quad (4)$$

Substituting Eq.(4) in Eq.(1)

$$J \frac{d^2 \delta_m}{dt^2} = T_a = T_m - T_e \quad (5)$$

$$\text{Since } \omega_m = d \theta_m / dt \quad (6)$$

Then by substituting Eq. (6) in Eq. (1) we obtain

$$J \omega_m \frac{d^2 \delta_m}{dt^2} = P_a = P_m - P_e \quad \text{Watt} \quad (7)$$

where

P_m is the shaft power supplied by the prime mover

P_e is the electrical power output

P_a is the accelerating power which accounts for any unbalance between those two quantities

$J \omega_m$ is the angular momentum of the rotor and at synchronous speed ω_{sm} it is given by the symbol M which is measured in J.s /rad. And thus Eq. (7) can be written as follows

$$M \frac{d^2 \delta_m}{dt^2} = P_a = P_m - P_e \quad (8)$$

Defining the inertia constant as

$$H = \frac{\text{stored kinetic energy in megajoules at synchronous speed}}{\text{machine rating in MVA}}$$

$$\text{and } H = \frac{\frac{1}{2} J \omega_{sm}^2}{S_{mach}} = \frac{\frac{1}{2} M \omega_{sm}}{S_{mach}} \quad \text{MJ / MVA} \quad (9)$$

$$\text{Thus, } M = \frac{2H}{\omega_{sm}} S_{mach} \quad \text{MJ / mech rad} \quad (10)$$

Substituting for M in Eq.(8) we obtain

$$\frac{2H}{\omega_{sm}} \frac{d^2 \delta_m}{dt^2} = \frac{P_a}{S_{mach}} = \frac{P_m - P_e}{S_{mach}} \quad (11)$$

Expressing the formula in per unit it can be written as follows

$$\frac{2H}{\omega_s} \frac{d^2 \delta_m}{dt^2} = P_a = P_m - P_e \quad \text{per unit} \quad (12)$$

Taking into consideration that ω_s and δ are expressed in the same units, whether mechanical or electrical radians or degrees. H and t are in seconds. $P_a, P_m,$ and P_e are in per unit with the same base as H . ω_s is the synchronous speed in electrical units. Equation (12) is known as the swing equation of the machine and it is the basic equation in stability studies for representing the rotational dynamics of the synchronous machines. It is 2nd order differential equation and it can be expressed as two 1st order differential equations as follows

$$\frac{2H}{\omega_s} \frac{d\omega}{dt} = P_m - P_e \quad \text{per unit} \quad (13)$$

$$\frac{d\delta}{dt} = \omega - \omega_s \quad (14)$$

where $\omega, \omega_s,$ and δ are in electrical degrees or radians.

The swing equation is solved to determine the stability of a machine in a power system [37].

3.2. Proposed System

The IEEE 9 bus system is simulated using the OpenModelica open source software, the circuit is constructed using the OpenModelica components as depicted in Fig. 2. The IEEE 9 bus system is composed of 9 buses, 6 lines (line 45, line56, line 67, line78, line 89, and line49), 3 transformers, 3 loads (at buses 5, 7, and 9), and 3 generators (buses 1, 2, and 3) [40].

The components are organized and connected using drag and drop from the appropriate libraries; from Open iTesla Power System Library (OpenIPSL), as well as from a Technical University of Delft library named DelMod. The square added in the upper left corner of the circuit presented in Fig. 2 is a system base card that provides the base values for the frequency and the apparent power in Mega Volt Ampere (MVA) of the system.

The generator was the only component that was built as a separate model. It is constructed as a 4th order generator and represented with a customized icon; afterwards, it was connected to the rest of the IEEE system components. It is noted that all the loads are voltage-dependent loads except for load 7 which is a scaled load with a step input at $t = 50$ s of the simulation. This step input simulates an increase in the load at the 50th second.

For the analysis, the connections of the components are checked before the simulation is run. Afterwards, a simulation for 150 seconds of the test system is run to investigate the impact of the increase in load due to step input. The voltages of the 3 buses connected to the generators are plotted. Moreover, the frequencies (rotor speed) of the 3 generators are also plotted.

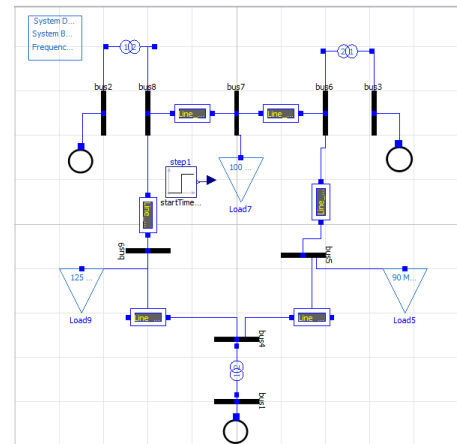


Fig. 2. IEEE 9 bus system in OpenModelica

A simulation output window is obtained when the 150 seconds simulation is finished, as shown in Fig. 3. Once the simulation is finished, we are directed to a plot area to visualize the results. Results obtained can be plotted in the plot area shown in Fig. 3, and different parameters can be saved as a .csv sheet and plotted using other tools.

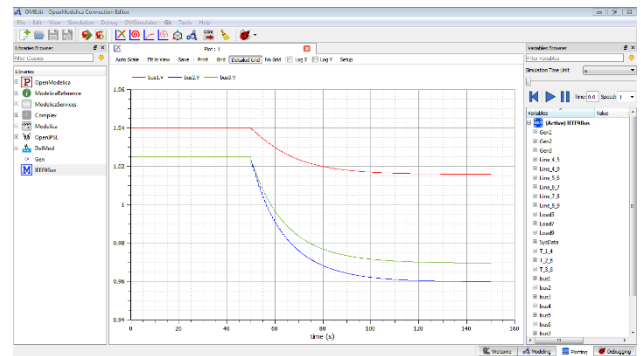


Fig. 3. IEEE 9 bus system finished simulation interface

To add the controllers, the previously constructed 4th order generator model is adjusted. First, an automatic voltage regulator (AVR) is connected to the generator as depicted in Fig. 4 and the system behavior observed. Afterwards, a speed governor (GOV) controller is used in addition to the AVR as illustrated in Fig. 5 and the system behavior is again observed. For the analysis, a simulation of 150 seconds is run to investigate the impact of the increase in load 7 due to the step input introduced at $t = 50$ seconds with and without using the AVG and GOV controllers. The voltages of the 3 buses connected to the generators are plotted in Fig. 6. Moreover, the frequencies (rotor speed) of the 3 generators are also plotted in Fig. 7 with and without using controllers.

3.3. Model analysis using AVR and GOV controllers - Generators bus voltages

The values of the voltages for bus 1, bus 2, and bus 3 are saved as .csv and then plotted. Figure 6 depicts the voltage values for the system first when no controllers are used (a), then when AVR is used (b), and finally when both controllers AVR and GOV are used. The voltages in per unit are plotted against the simulation time in seconds.

It is observed that a rise in the load value, introduced by the step input to the scaled load 7 at $t = 50$ seconds caused a drop in the voltage at the generators buses when no controllers are used as presented in Fig. 6(a). This drop is observed until the end of the simulation time (150 sec), reaching minimum values of 1.0158 p.u (16.11 V), 0.9597 p.u. (16.85 V), and 0.9695 p.u. (13.05 V) for the three buses 1, 2, and 3, respectively. It is also observed that V_1 has a different higher initial value than V_2 and V_3 , where its curve starts at the higher initial value of 1.04 p.u. rather than 1.025 p.u. for V_2 and V_3 .

The rationale for this is that the amount of power generated from the generators in the network is fixed $P = V \times I$. As the load increases (load 7 via step input) the current I drawn by the load increases accordingly. As the power is maintained constant and is not increased, a constant P with the increase in current (I) implies a drop in the voltage (V) as observed.

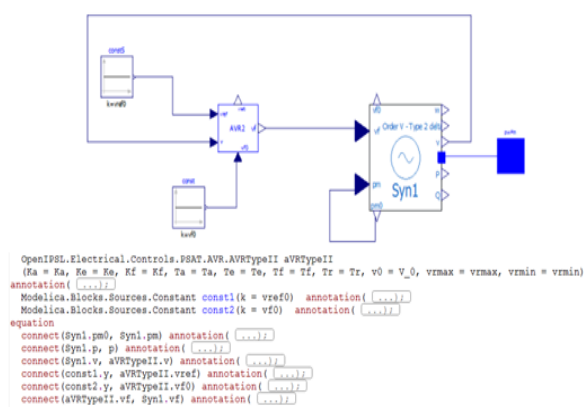


Fig. 4. The generator Modelica model with AVR controller added

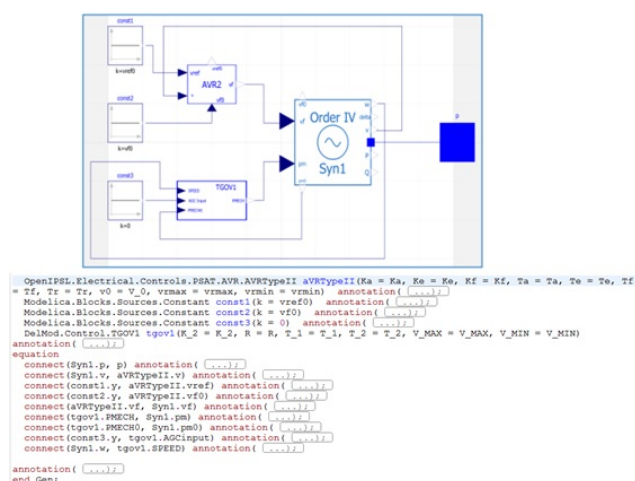


Fig. 5. The generator Modelica model with AVR and GOV controllers added

When the AVR is introduced the voltage drop, caused by load increase, occurred transiently for few seconds with a few oscillations, and then the pre-disturbance values of the voltage at the 3 buses are retained once more as illustrated in Fig. 6(b). In Fig. 6(c) where both the AVR and the GOV controllers are connected, it is observed that the voltage drop and oscillations

due to the load increase are more in amplitude and duration than the previous case with no GOV controller. After oscillating for a few seconds again the voltage values at the three buses are returned to their pre-disturbance values. The AVR adjusts the output voltage of the generator by comparing it to a reference value, and the difference, which is the error, is compensated for by controlling the generator excitation field current.

3.4. Model analysis using AVR and GOV controllers - Generator bus frequencies

The values of the frequencies are investigated through investigating the generators rotor speed (ω) as

$$f = \frac{p}{120} \cdot \omega \quad (15)$$

Where P is the number of poles and ω is the rotor speed in rpm.

Thus, for Gen 1, Gen 2, and Gen 3, the rotor speed values are saved as .csv and then plotted as depicted in Fig. 7. The values in per unit are plotted against the simulation time in seconds. It is observed in Fig. 7 (a) without using controllers, that a rise in the load value, introduced by the step input to the scaled load 7 at $t = 50$ seconds caused a drop in the frequencies at the generators buses, i.e. generators rotor speed reaching minimum values of 0.946002 p.u (47.3001 Hz), 0.946004 p.u. (47.3002 Hz), and 0.946003 p.u. (47.30015 Hz) for the three buses 1, 2, and 3 respectively.

The drop is observed until around $t = 100$ seconds. Afterwards, the rotor speed started to rise, but it did not return to its nominal value before the end of the simulation time (150 sec). From Fig. 6 (a) the values of the voltages at these buses started to stabilize also around $t = 100$ seconds, and no more reduction in the voltage values are observed.

The power is supplied by the stored kinetic energy of the rotor represented in the form of real power P as follows

$$K = \frac{1}{2} I \cdot \omega^2 \quad (16)$$

where I is the inertia and ω is the rotor speed in rpm.

When the load increases more torque is needed from the generator side, if not supplied and as the mass of the rotor is constant, with the increase in load its stored kinetic energy starts to drop, thus the rotor speed ω also drops.

The drop of frequency is also observed when the AVR controller is connected to the generator, as presented in Fig. 7(b). The GOV controller addition improved the response of the frequency of the system as shown in Fig. 7(c).

Figure 7(c) illustrates the drop and oscillations of the frequency starting at the 50th second; afterwards, steady-state is obtained and the frequency stabilizes. The drop and fluctuations are observed until about $t = 90$ seconds.

Afterwards, the rotor speed started to stabilize again, but it does not return to its nominal value (pre-disturbance value) before the end of the simulation time (150 sec).

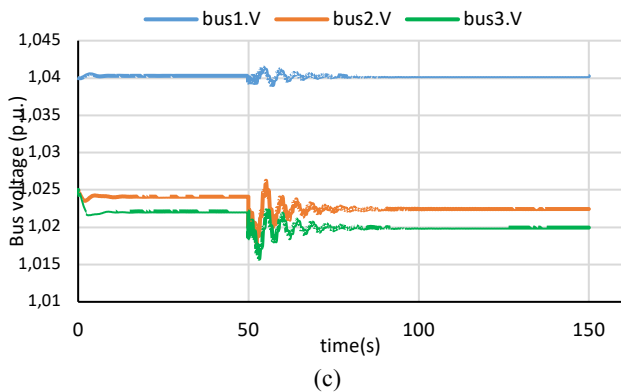
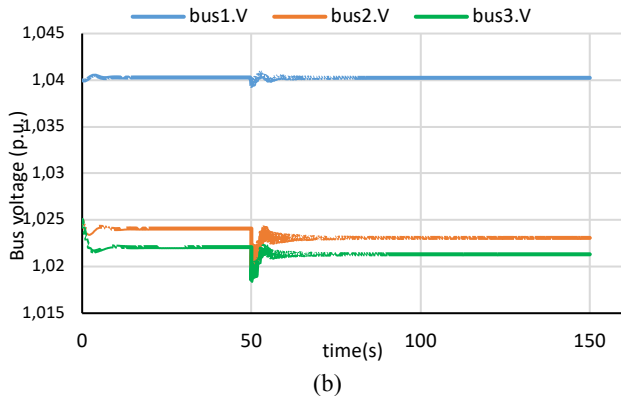
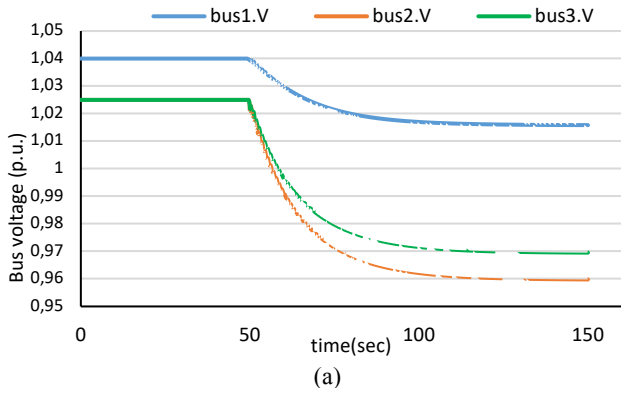


Fig. 6. Generators buses voltages (a) Using no controllers (b) Using AVG controller (c) Using AVG + GOV controllers

From Fig. 6 (b) and Fig. 6 (c) the values of the voltages at these buses started to stabilize around $t = 90$ seconds, and no more fluctuations in the voltage values are observed. The 3 generators speed curves coincide as they are identical and working at the same nominal frequency value 50 Hz.

The generator mechanical power is not a function of frequency. During steady-state continuous operation, the GOV controller is used to adjust the mechanical output power without varying the frequency. On the other hand, the load active power is frequency dependent. An increase in load power causes a reduction in frequency and vice versa. In other words, the power is inversely proportional to the frequency i.e. $P \propto \frac{1}{f}$. The GOV controller is thus used to maintain a constant speed and accordingly constant frequency via controlling the prime mover fuel.

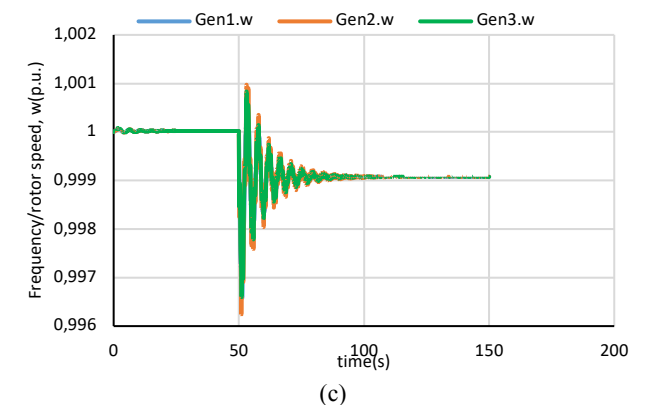
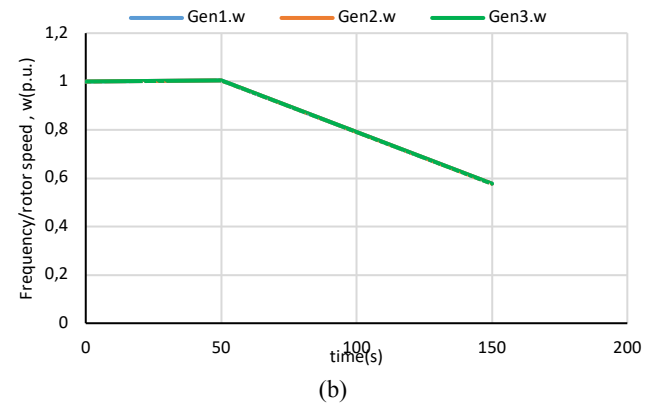
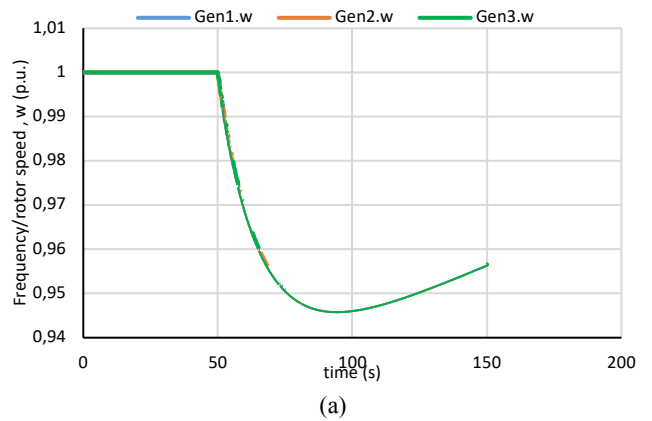


Fig. 7. Generators rotor speeds (frequencies) (a) Using no controllers (b) Using AVG controller (c) Using AVG + GOV controllers

4. Model analysis with wind turbine integration

In this section, the IEEE 9 bus system constructed and simulated in section 2 is once more simulated here, adding a renewable energy resource, which is a wind turbine. The circuit used is depicted in Fig. 8, where the wind turbine is connected to bus 12.

For the analysis, a simulation for 100 seconds of the system is run to investigate the impact of the integration of the wind turbine into bus 12 of the system.

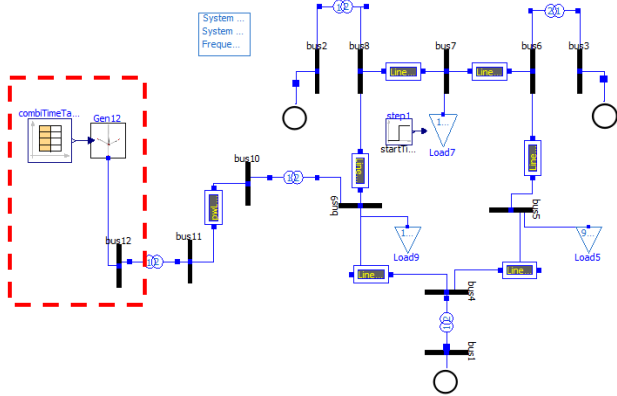


Fig. 8. IEEE 9 bus system with integrated wind turbine modelled in OpenModelica

First, an assumption of constant wind speed is used for the analysis. Afterwards, variable wind speed is fed to the wind turbine for the analysis. For both cases, the output power of the 3 generators and the wind turbine are plotted. Also, the voltages of the wind turbine bus, as well as the 3 buses connected to the generators, are plotted. Moreover, the frequencies (rotor speed) of the 3 generators are also plotted.

4.1. Constant Wind Speed

A constant wind speed of 19 m/s is fed to the wind turbine connected to bus 12 using a constant block with $k=19$. Figure 9 depicts the real power of the wind turbine at bus 12 and the 3 generators. It is shown that minimal oscillations are observed for power generated from the 3 generators at the beginning of the simulation. This is rapidly restored, as this system has 2 controllers, the AVR and the GOV. The impact of the AVR controller is illustrated in Fig. 10 where the voltages of the buses 1, 2, 3, and 12 are returned to their initial values and stabilize around the 30th second after experiencing the fluctuations at the start. As elaborated earlier, the values of the frequencies are investigated through studying the generator rotor speeds (ω). These are plotted in Fig. 11 and the oscillations experienced at the start are controlled and returned to a stable constant value around the 40th second via the GOV speed controller. The 3 generator speed curves coincide as they are identical and working at the same nominal frequency value of 50 Hz.

4.2. Variable Wind Speed

A text file is used to input varied wind speed values to the wind turbine connected at bus 12, simulating a more realistic scenario. The wind speed takes variable speed values with a maximum value of 21.3 m/s and a minimum value of 11.5 m/s. The function relating wind turbine power to wind speed is given by $P = \frac{1}{2} \rho A v^3 C_p$ (17)

Where ρ is the air density in kg/m^3 , A is the area swept by the blade in m^2 , v is the wind speed, and C_p is the power coefficient of performance.

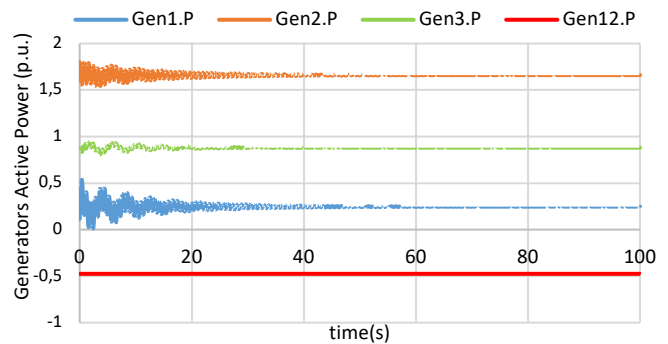


Fig. 9. Generators real power output of the IEEE 9 bus system with constant speed wind turbine

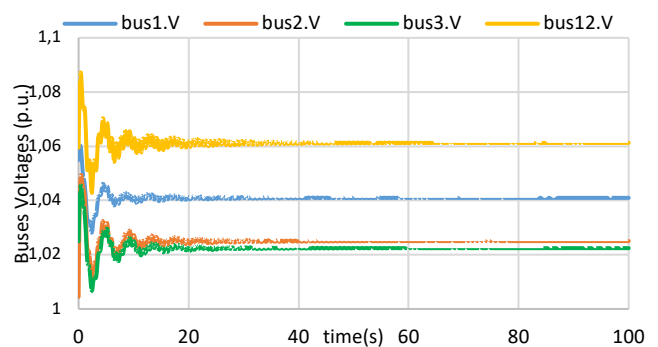


Fig. 10. Generators buses voltages of the IEEE 9 bus system with integrated constant speed wind turbine

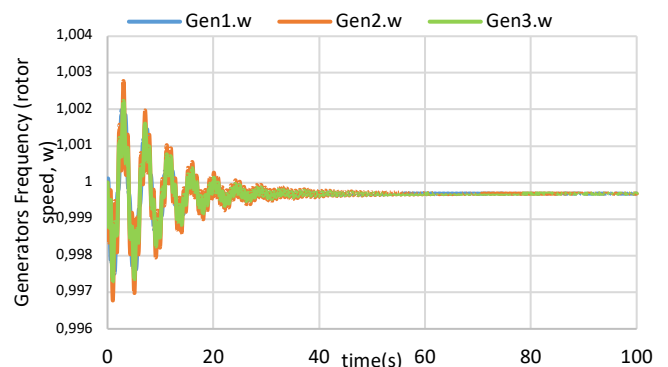


Fig. 11. Generators rotor speeds (frequencies) of the IEEE 9 bus system with integrated constant speed wind turbine

This formula implies that the wind turbine available output power is directly proportional to the wind speed cubed.

This is depicted in Fig. 12 where the turbine active power varies according to the variation of the input wind speed. Figure 13 shows the real output power of the 3 generators in the system, illustrating how the variation in wind speed affects the output power, where distortion is noticed in the values of the output power of the 3 generators throughout the whole simulation duration (100 s). Afterwards, it is illustrated in Fig. 14 and Fig. 15 how the voltage and the frequency of the generators, respectively, are affected by the wind speed variation. The distortion of the voltage and frequency are noticed during the simulation period, rather than stabilizing

after a few seconds as shown in the previous constant wind speed case.

4.3. Analysis of the Wind Turbine Power Voltage dependency

The wind turbine power dependency on the terminal voltage are represented as follows

$$P = P_o V^{\alpha_{phap}} \quad Q = Q_o V^{\alpha_{phaq}} \quad (18)$$

Relating Eq. (17) and Eq. (18), it can be noted that as the wind speed increases higher levels of voltage are to be generated [41]. To investigate the voltage dependency of the wind turbine active and reactive power to the terminal voltage, the system was simulated using different values of the parameters α_{phap} and α_{phaq} in a step of 0.5 and the behavior of the system was plotted. Figure 16 presents the voltage of the wind turbine for different values of α_{phap} and α_{phaq} .

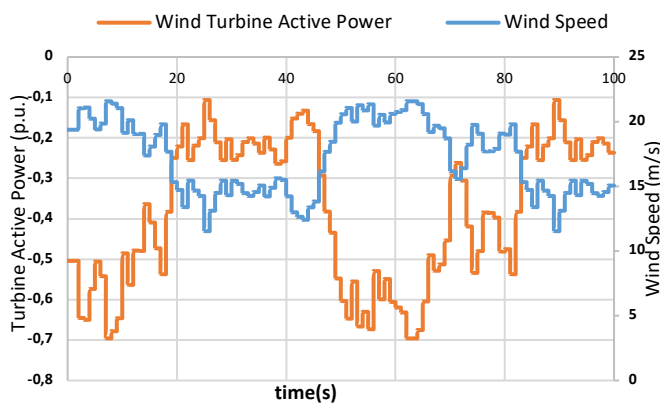


Fig. 12. Real output power of the wind turbine connected to the IEEE 9 bus system for varying wind speed

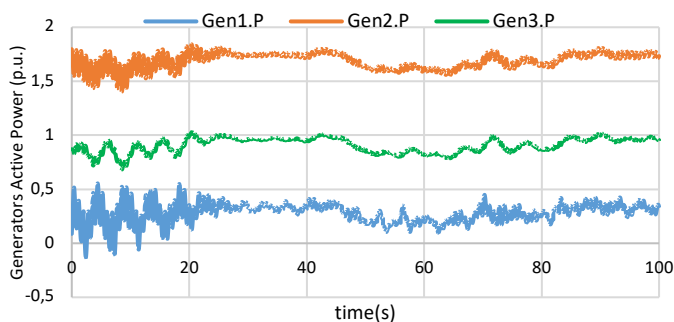


Fig. 13. Real output power of the generators of the IEEE 9 bus system with varying speed wind turbine

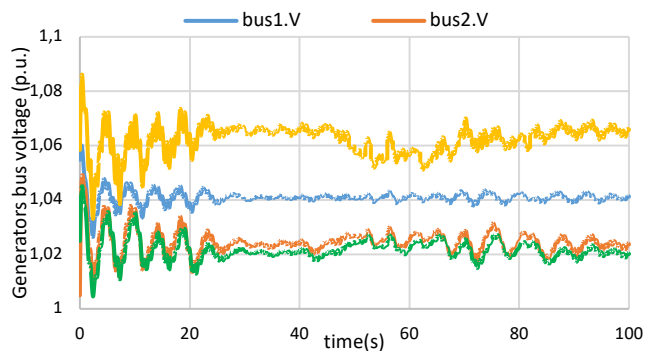


Fig. 14. Bus voltages for the generators of the IEEE 9 bus system with integrated wind turbine at varying wind speed

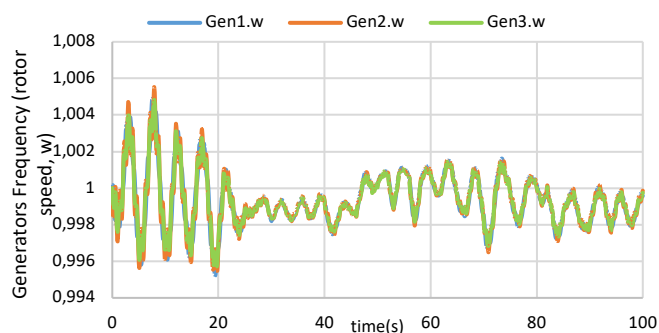


Fig. 15. Generators rotor speeds (frequencies) of the IEEE 9 bus system with integrated varying speed wind turbine

It is noted that an increase in the α_{phap} and α_{phaq} parameters causes minimal reduction in voltage values. Fig. 17 depicts the wind turbine active power, where it may be seen that an increase in α_{phap} and α_{phaq} values causes a significant increase in the active power values with an average increase rate of 12.15% from $\alpha = 0$ to $\alpha = 2$. Figure 18 illustrates the wind turbine reactive power, again an increase in α_{phap} and α_{phaq} resulted in a significant increase of the reactive power values with an average increase rate of 12.15% from $\alpha = 0$ to $\alpha = 2$. As α_{phap} and α_{phaq} have similar values they are referred to in the figures as 1 parameter, α .

For the computation time, the OpenModelica software is used to simulate the IEEE 9 bus system with an integrated wind turbine on an Intel® Core™ i7 @ 1.73 processor with a 4 GB installed memory on a 64-bit MS Windows® operating system. It is worth noting that 2 iterations of runs were implemented on the same system and the results are recorded in Table 1. From Table 1 it is observed that for a value of α greater than 0 the computation time is larger than that used for the case when α equals 0, but the discrepancy is in the range of few seconds. The computational time is highest for [2,2], and lowest for the [1,1] case of α_{phap} and α_{phaq} .

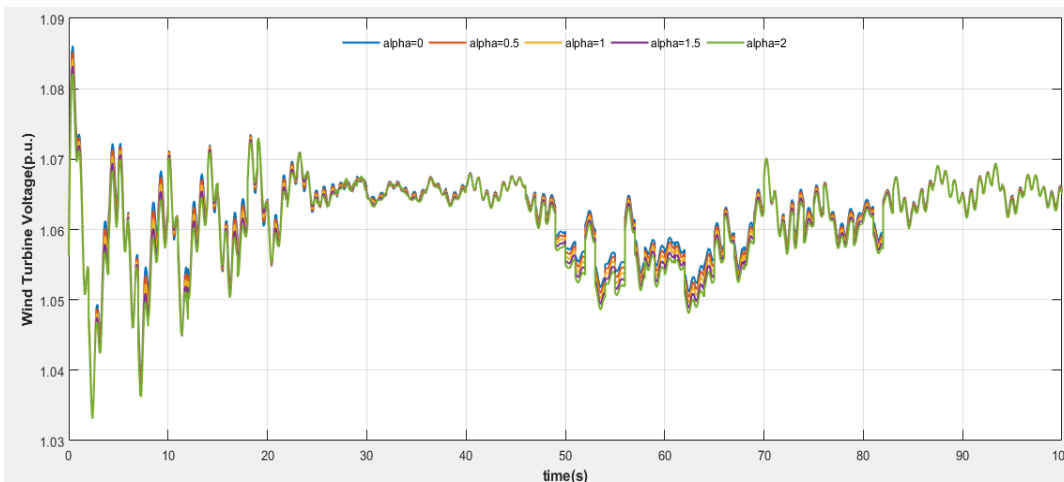


Fig. 16. Wind turbine bus voltages for different values of α and α at varying wind speed

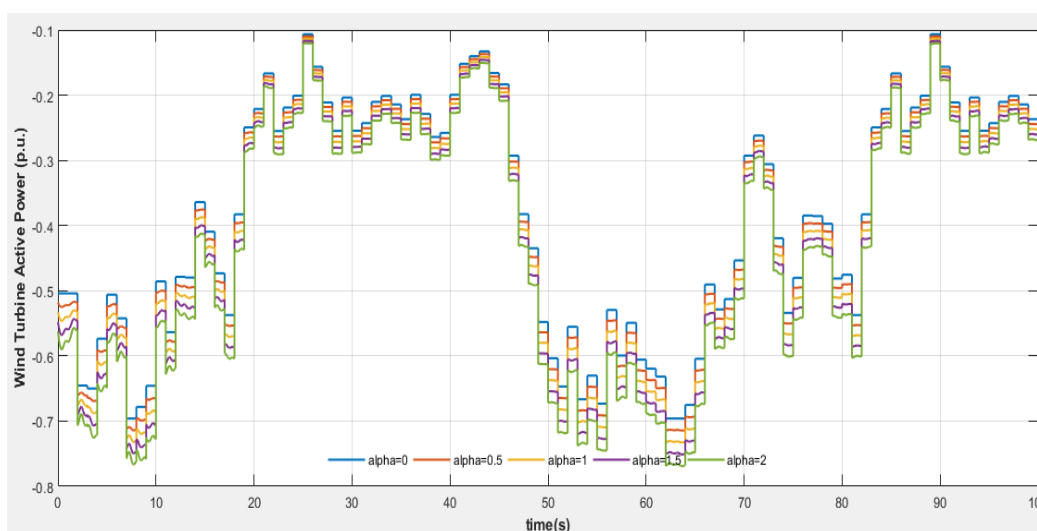


Fig. 17. Wind turbine active power for different values of α and α at varying wind speed

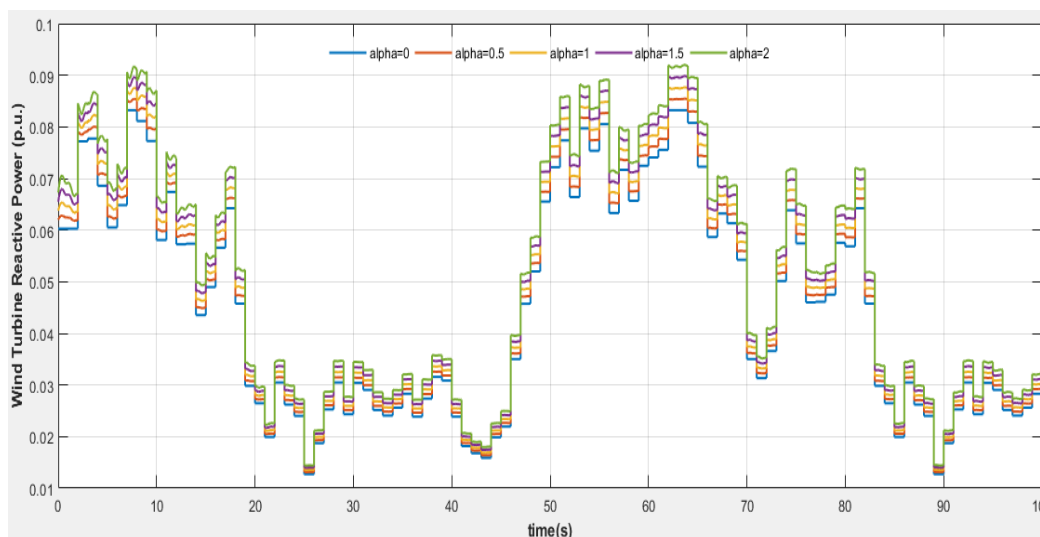


Fig. 18. Wind turbine reactive power for different values of α and α at varying wind speed

5. Conclusions

This paper aims to present how to use an open-source software to model a standard power network, and to perform

a steady-state analysis while integrating a wind turbine into the network. The IEEE 9 bus system is simulated using the OpenModelica software.

First, the steady-state stability of the system is analyzed with and without controllers. It was concluded that

introducing an increase in the load at bus 7 caused a decrease in bus voltages in the network. And the same goes for the drop in frequency (rotor speed) of the generators, which is expected when the generation is less than the required power to be supplied to the load. Thus, the AVR is used to maintain the voltage values at generator buses to their initial pre-disturbance values by controlling the generator excitation field current. The GOV maintains the speed of the generator constant, and accordingly the frequency, by controlling fuel fed to the prime mover. In this study, to alleviate reduction in frequency due to load increase, the fuel of the prime mover was increased.

Afterwards, the steady-state stability is investigated when integrating a wind turbine into the IEEE 9 bus system. It was concluded that a distortion of the system voltage profile and frequency occurred when integrating renewable energy generators, specifically a wind turbine. This is mainly due to the variability of the natural energy resource. A comparison is performed between a scenario with assumed constant wind speed and a more realistic scenario with variable wind speed. It was observed that the variability of wind speed is the reason for the distortion obtained when integrating a wind turbine at bus 12 in the IEEE 9 bus system. The power generated from a wind turbine is directly proportional to the cube of the wind velocity. When considering the voltage dependency of the wind turbine power, it is noted that as the dependency increases (increased values of α_p and α_q parameters) the wind turbine generated real and reactive power increase. Moreover, the computation time also increases with the increase in dependency due to the increase in complexity of the formulas governing the wind turbine power voltage dependencies.

The open-source software OpenModelica application in this study proved to be a user friendly, efficient software that is capable of modelling and analyzing a power system network in a timely manner. The authors intend to apply the software for simulating larger systems in the future to investigate its capability to handle real-life large power systems. Moreover, the authors plan to perform a comparative study with graph trace analysis [42].

Table 1. Computation time for running the IEEE 9 bus system with wind turbine at different values of α_p and α_q (α)

α	0	0.5	1	1.5	2
iter 1 time (s)	74.26	77.55	77.2	79.12	79.34
iter 2 time (s)	74.88	78.4	76.96	79.16	88.1

References

[1] GWEC, "Global Wind Energy Council (GWEC) 2019 Global Wind Annual Report," Brussels, Belgium 2019.
 [2] D. X. He and Y. Li, "Overview of Worldwide Wind Power Industry," in *Strategies of Sustainable Development in China's Wind Power Industry*, ed Singapore: Springer Singapore, 2020, pp. 29-60.

[3] A. Ameer, K. Loudiyi, and M. Aggour, "Steady State and Dynamic Analysis of Renewable Energy Integration into the Grid using PSS/E Software," *Energy Procedia*, vol. 141, pp. 119-125, 2017.
 [4] J. C. Li and D. X. He, "Innovation Fields for Sustainable Development of Wind Power," in *Strategies of Sustainable Development in China's Wind Power Industry*, ed Singapore: Springer Singapore, 2020, pp. 223-392.
 [5] D. Q. Hung, M. R. Shah, and N. Mithulananthan, "Technical Challenges, Security and Risk in Grid Integration of Renewable Energy," in *Smart Power Systems and Renewable Energy System Integration*, D. Jayaweera, Ed., ed Cham: Springer International Publishing, 2016, pp. 99-118.
 [6] H. Tazvinga, M. Thopil, P. B. Numbi, and T. Adefarati, "Distributed Renewable Energy Technologies," in *Handbook of Distributed Generation: Electric Power Technologies, Economics and Environmental Impacts*, R. Bansal, Ed., ed Cham: Springer International Publishing, 2017, pp. 3-67.
 [7] T. Sharma and O. Singh, "Voltage Stability Analysis of Wind Integrated Grid," in *International Conference on Intelligent Computing and Smart Communication 2019*, 2020, pp. 857-866.
 [8] A. Kunwar, R. Bansal, and O. Krause, "Steady-state and transient voltage stability analysis of a weak distribution system with a remote doubly fed induction generator-based wind farm," *Energy Science & Engineering*, vol. 2, pp. 188-195, 2014.
 [9] M. M. Aly and M. Abdel-Akher, "Voltage stability assessment for radial distribution power system with wind power penetration," presented at the IET Conference on Renewable Power Generation (RPG 2011) Edinburgh, UK, 2011.
 [10] E. Bekiroglu and M. D. Yazar, "Analysis of Grid Connected Wind Power System," in *2019 8th International Conference on Renewable Energy Research and Applications (ICRERA)*, 2019, pp. 869-873.
 [11] Z. Xu, C. Yunlong, W. Yixian, Z. Xiaobing, C. Xueting, and G. Lei, "Reactive-voltage Partitioning Method for Wind Power Grid Based on Interval Uncertainty Clustering," in *2019 IEEE Sustainable Power and Energy Conference (iSPEC)*, 2019, pp. 353-358.
 [12] W. Wei and J. Wang, "Electric Power System with Renewable Generation," in *Modeling and Optimization of Interdependent Energy Infrastructures*, ed Cham: Springer International Publishing, 2020, pp. 21-161.
 [13] S. Favuzza, M. N. Navia, R. Musca, E. R. Sanseverino, G. Zizzo, B. D. Van, *et al.*, "Impact of RES Penetration on the Frequency Dynamics of the 500 kV Vietnamese Power System," in *2019 8th International Conference on Renewable Energy Research and Applications (ICRERA)*, 2019, pp. 668-672.

- [14] A. Shahid, "Smart grid integration of renewable energy systems," in *2018 7th International Conference on Renewable Energy Research and Applications (ICRERA)*, 2018, pp. 944-948.
- [15] B. Banerjee, D. Jayaweera, and S. Islam, "Grid Integration of Renewable Energy Systems," in *Smart Power Systems and Renewable Energy System Integration*, D. Jayaweera, Ed., ed Cham: Springer International Publishing, 2016, pp. 75-97.
- [16] M. Lawan, M. Camara, J. Raharijaona, and B. Dakyo, "Wind turbine and batteries with variable speed Diesel generator for micro-grid applications," in *2018 7th International Conference on Renewable Energy Research and Applications (ICRERA)*, 2018, pp. 897-901.
- [17] Y. Yang, S. Lin, Q. Wang, Y. Xie, and M. Liu, "Multi-objective optimal control approach for static voltage stability of power system considering interval uncertainty of the wind farm output," *IEEE Access*, 2020.
- [18] W. Du, W. Dong, and H. F. Wang, "Small-Signal Stability Limit of a Grid-Connected PMSG Wind Farm Dominated by the Dynamics of PLLs," *IEEE Transactions on Power Systems*, vol. 35, pp. 2093-2107, 2019.
- [19] B. B. Adetokun, C. M. Muriithi, and J. O. Ojo, "Voltage stability assessment and enhancement of power grid with increasing wind energy penetration," *International Journal of Electrical Power & Energy Systems*, vol. 120, p. 105988, 2020.
- [20] S. Kumar, A. Kumar, and N. Sharma, "A novel method to investigate voltage stability of IEEE-14 bus wind integrated system using PSAT," *Frontiers in Energy*, vol. 14, pp. 410-418, 2020.
- [21] S. Essallah, A. Bouallegue, and A. Khedher, "Integration of automatic voltage regulator and power system stabilizer: small-signal stability in DFIG-based wind farms," *Journal of Modern Power Systems and Clean Energy*, vol. 7, pp. 1115-1128, 2019.
- [22] E. Rakhshani, D. Gusain, V. Sewdien, J. L. R. Torres, and M. A. Van Der Meijden, "A key performance indicator to assess the frequency stability of wind generation dominated power system," *IEEE Access*, vol. 7, pp. 130957-130969, 2019.
- [23] A. Sajadi, S. Zhao, K. Clark, and K. A. Loparo, "Small-Signal Stability Analysis of Large-Scale Power Systems in Response to Variability of Offshore Wind Power Plants," *IEEE Systems Journal*, vol. 13, pp. 3070-3079, 2018.
- [24] A. Sajadi, R. M. Kolacinski, K. Clark, and K. A. Loparo, "Transient stability analysis for offshore wind power plant integration planning studies—Part I: Short-term faults," *IEEE Transactions on Industry Applications*, vol. 55, pp. 182-192, 2018.
- [25] A. Sajadi, R. M. Kolacinski, K. Clark, and K. A. Loparo, "Transient stability analysis for offshore wind power plant integration planning studies—Part II: Long-term faults," *IEEE Transactions on Industry Applications*, vol. 55, pp. 193-202, 2018.
- [26] M. B. Wafaa and L.-A. Dessaint, "Approach to dynamic voltage stability analysis for DFIG wind parks integration," *IET Renewable Power Generation*, vol. 12, pp. 190-197, 2017.
- [27] L. Gan, G. Li, and M. Zhou, "Coordinated planning of large-scale wind farm integration system and regional transmission network considering static voltage stability constraints," *Electric Power Systems Research*, vol. 136, pp. 298-308, 2016.
- [28] J. Xu, P. K. Kanyingi, K. Wang, G. Li, B. Han, and X. Jiang, "Probabilistic small signal stability analysis with large scale integration of wind power considering dependence," *Renewable and Sustainable Energy Reviews*, vol. 69, pp. 1258-1270, 2017.
- [29] Y. Krim, S. Krim, and M. F. Mimouni, "Control of a wind farm connected to the grid at a frequency and variable voltage," *International Journal Of Renewable Energy Research, IJRRER*, vol. 6, 2016.
- [30] M. Taherkhani, S. H. Hosseini, M. S. Javadi, and J. P. Catalão, "Scenario-based probabilistic multi-stage optimization for transmission expansion planning incorporating wind generation integration," *Electric Power Systems Research*, vol. 189, p. 106601, 2020.
- [31] A. Gholizadeh, A. Rabiee, and R. Fadaeinedjad, "A scenario-based voltage stability constrained planning model for integration of large-scale wind farms," *International Journal of Electrical Power & Energy Systems*, vol. 105, pp. 564-580, 2019.
- [32] S. D. Ahmed, F. S. Al-Ismaïl, M. Shafiullah, F. A. Al-Sulaiman, and I. M. El-Amin, "Grid integration challenges of wind energy: A review," *IEEE Access*, vol. 8, pp. 10857-10878, 2020.
- [33] X. Yuan, "Overview of problems in large-scale wind integrations," *Journal of Modern Power Systems and Clean Energy*, vol. 1, pp. 22-25, 2013.
- [34] A. Harrouz, I. Colak, and K. Kayisli, "Energy Modeling Output of Wind System based on Wind Speed," in *2019 8th International Conference on Renewable Energy Research and Applications (ICRERA)*, 2019, pp. 63-68.
- [35] S. Sakurai, O. Sakamoto, and T. Nitta, "Linearized Model of Power System with Synchronous Generator, Variable Renewable Energy Generation and Load," in *2019 8th International Conference on Renewable Energy Research and Applications (ICRERA)*, 2019, pp. 276-279.
- [36] P. Fritzson, A. Pop, A. Asghar, B. Bachmann, W. Braun, R. Braun, *et al.*, "The OpenModelica Integrated Modeling,

Simulation and Optimization Environment," in *Proceedings of the 1st American Modelica Conference*, 2018, pp. 8-10.

[37] J. J. Grainger, W. D. Stevenson, and W. D. Stevenson, *Power system analysis*, 2003.

[38] P. Murty, *Power systems analysis*: Butterworth-Heinemann, 2017.

[39] T. Nagsarkar and M. Sukhija, *Power system analysis*: Oxford University Press, 2014.

[40] MHI, "PSCAD IEEE 09 Bus System," Manitoba Hydro International, Canada2018.

[41] C. P. Chatchai Promdee, "Effects of wind angles and wind speeds on voltage generation of savonius wind turbine with double wind tunnels," *Procedia Computer Science* vol. 86, pp. 401-404, 2016.

[42] A. Tbaileh, H. Jain, R. Broadwater, J. Cordova, R. Arghandeh, and M. Dilek, "Graph Trace Analysis: An object-oriented power flow, verifications and comparisons," *Electric Power Systems Research*, vol. 147, pp. 145-153, 2017.